Reconfigurable Range-Doppler Processing and Range Resolution Improvement for FMCW Radar

Neemat, Sharef; Uysal, Faruk; Krasnov, Oleg; Yarovoy, Alexander

DOI
10.1109/JSEN.2019.2923053

Publication date
2019

Document Version
Final published version

Published in
IEEE Sensors Journal

Reconfigurable Range-Doppler Processing and Range Resolution Improvement for FMCW Radar

Sharef Neemat, Faruk Uysal, *Senior Member, IEEE*, Oleg Krasnov, and Alexander Yarovoy, *Fellow, IEEE*

***Abstract*— A reconfigurable range-Doppler processing method for FMCW radar is presented. By concatenating beat-frequency signals from more than one sweep, a continuous beat-frequency signal for the whole coherent processing interval (CPI) can be created. As a result, continuous targets' observation time is extended beyond that of a single chirp duration, leading to range resolution improvement. The created continuous beat-frequency signal can be split in the digital domain to any two-dimensional slow-time and fast-time matrices with the same number of elements as in the original signals, which offers a realization of a software-defined pulse/sweep repetition rate in range-Doppler processing. The signal concatenation is done in the short-time Fourier transform (STFT) domain, where the beat-frequency slices are extrapolated to compensate for the observation time lost in the transient region between sweeps, and then a phase correction is applied to each frequency-slice as appropriate, followed by an inverse STFT (ISTFT). The proposed technique is verified with simulation and experiments with an FMCW radar for stable and moving target scenarios. We found that the method allows for range resolution improvement without the transmission of additional bandwidth and also allows for the ability to observe different resolution granularities in parallel from one CPI. It additionally allows the decoupling of the transmitted PRF from the Doppler processing PRF, permitting the facility to observe different unambiguous Doppler velocity intervals from one CPI, without compromising on the total CPI processing gain.**

***Index Terms*— Beat-frequency, coherent processing interval (CPI), frequency-modulated continuous-wave (FMCW), range resolution, unambiguous Doppler velocity.**

I. Introduction

DERAMPING Frequency Modulated Continuous Wave (FMCW) radars operate by mixing a transmitted chirp signal with received returns, and filtering the resulting beat signal [1]. For a single point-target, the time delay between the probing signal transmission and the scattered signal reception will result in a single-tone signal, known as a beat-frequency, whose frequency is proportional to that target's range. Range is therefore defined by frequency. The scaling between beat-frequencies and range is defined by the transmitted bandwidth, and the signal observation time. A frequency estimation technique like the Fourier Transform (FT) is typically used to separate targets in range, by separating beat-frequency tones in the frequency domain. The radar's range resolution is determined by the transmitted bandwidth and the FT frequency spectrum resolution. Legacy computer architectures used in FMCW radars are highly compatible with the FT for its reduced computational requirements and predictable latency. The range resolution granularity defines the width of targets' range bins. In signal processing, the FT frequency resolution is defined by the signal observation time [2]. Target velocities are calculated from Doppler processing - also typically using the FT - across targets' range bins from multiple sweeps [3]. The radar Pulse/sweep Repetition Frequency (PRF) is therefore the Doppler sampling frequency. The time spent to gather multiple sweeps for range and Doppler processing is typically known as a Coherent Processing Interval (CPI). Sweeps in a CPI are typically arranged in a fast-time slow-time matrix, where fast-time is the time within a sweep, and slow-time is the time across multiple sweeps. The total processing gain in a CPI is contributed to the matrix's 2-D FT processing gain. It is typical for radars to transmit at different PRF values, across multiple CPIs to unambiguously determine targets' ranges and velocities, in what is known as staggered-PRF techniques [4]. In FMCW, the observation time is limited by what is known as the 'transient' or 'fly-back' region between frequency sweeps [5]. The received signal is typically only sampled after the transient region, which causes discontinuities in received beat-frequencies (demarking the end of a received sweep), and puts a limit on the possibility of having a continuous observation time.

The problem this paper offers a solution for is the existence of the transient regions in received beat-frequency sweeps in a CPI, in the sense that:

1) The existence of the transient regions does not allow for longer targets observations. If a method were to be developed to extend the observation time by coherently concatenating/processing beat-frequencies from more than one sweep at a time, that would result in a finer radar range resolution.
2) Such a concatenation method, would give a tool to decouple the Doppler processing PRF from the transmitted signal PRF. This is in the sense that it becomes possible to - in parallel and from one CPI - create different lengths fast-time slow-time matrices, without

Manuscript received April 23, 2019; revised June 4, 2019; accepted June 4, 2019. Date of publication July 2, 2019; date of current version September 18, 2019. The work of S. Neemat was supported by the KACST Scientific Institution. The associate editor coordinating the review of this paper and approving it for publication was Prof. Pai-Yen Chen. *(Corresponding author: Sharef Neemat.)*

The authors are with the Group of Microwave Sensing, Signals and Systems (MS3), Delft University of Technology, 2628CD Delft, The Netherlands (e-mail: s.a.m.neemat@tudelft.nl; f.uysal@tudelft.nl; o.a.krasnov@tudelft.nl; a.yarovoy@tudelft.nl).

Digital Object Identifier 10.1109/JSEN.2019.2923053

compromising on the total processing gain in any of the created matrices. This would therefore allow the implementation of staggered-PRF velocity disambiguation techniques in a single CPI.

The solution proposed in this paper is to concatenate beat-frequency slices in the Short-time Fourier Transform (STFT) domain, by applying a phase correction to each frequency slice as appropriate, followed by an Inverse STFT (ISTFT). A second optional realization of this solution is to first extrapolate beat-frequency slices, to compensate for the observation time lost in the transient region, then concatenate the slices as aforementioned.

Previous work on the topic is scarce, in the sense that a method doesn't exist where such a method:

- is applicable to deramping processing (as opposed to matched filtering),
- only relies on the FT (as opposed to more computationally intensive or iterative frequency estimation algorithms),
- does not improve the range resolution by stitches sweeps from multiple discontinuous bands, and therefore technically requiring more overall system bandwidth,
- does not require target detection as a prerequisite,
- is applicable to extended-targets.

Techniques that work by coherently processing data post range-Doppler may not be suitable for wide-band systems where range migration causes targets' energy to be spread across multiple range-Doppler bins. An interesting method for doubling the range resolution without increasing the bandwidth can be found in [6]. Their method is restricted to the radar's intermediate frequency being an integer multiple of the transmitted bandwidth, and to being operable only with a real Double-Side-Band (DSB) deramping receiver. Bandwidth extrapolation techniques like in [7]–[9] use prediction techniques to synthetically extrapolate the data to improve the resolution. There usually is a practical limit to how much will extrapolated data really represent target returns as associated with their Radar-Cross-Section (RCS). The work in [10] uses waveform diversity to decouple the Doppler cycle from the PRF, but does not address range resolution improvement. We proposed the extrapolation and linking of parts of beat frequencies - within the same sweep - in the STFT domain for the purpose of interference mitigation in [11].

The difference from previous techniques and the novelty in this work is highlighted in:

1) The first ever method for deramping FMCW radar sweeps coherent concatenation in the STFT domain.
2) The method allows for range resolution improvement without transmitting additional bandwidth.
3) The method offers the ability to observe different range resolution granularities in parallel from one CPI.
4) The method offers the ability to-in parallel-generate different size fast-time slow-time matrices, and decouples the transmitted PRF from the Doppler processing PRF, without compromising on the total CPI processing gain. This offers the ability to observer different unambiguous Doppler velocity intervals-to perform staggered PRF velocity-disambiguation techniques for example-in one CPI.
5) The method does not require target(s) detection as a prerequisite.

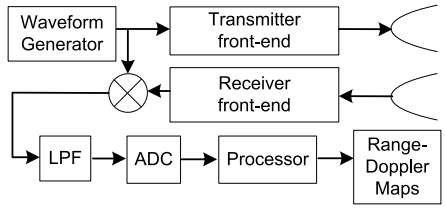

(a)

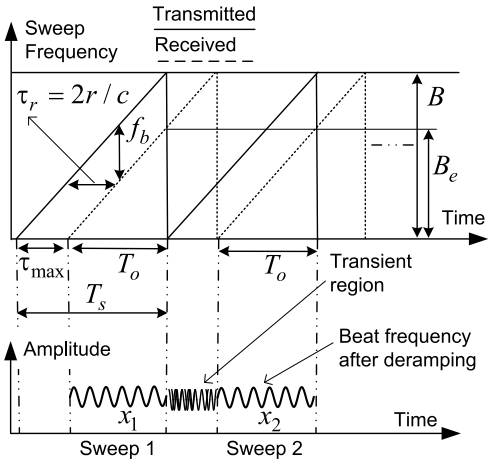

(b)

Fig. 1. (a) Deramping FMCW radar simplified block diagram. (b) Deramping operational overview, highlighting beat-frequency signals and the transient region.

II. Theory

A. Deramping FMCW Radar Range Resolution

A deramping FMCW radar - as in Fig. 1(a) - transmits bandwidth B over a sweep time T_s and observes a target at range r. The radar's Pulse Repetition Interval (PRI) is T_s. The observation time (ADC sampling interval) $T_o = (T_s - \tau_{\max})$, where $\tau_{\max}$ the maximum transient time [5], which is selected based the desired system maximum range of interest. The anti-aliasing Low Pass Filter (LPF) defines $\tau_{\max}$. The observation time T_o is less than T_s because it is limited by the transient time region from the previous sweep. ADC sampling of the received signal typically begins after $\tau_{\max}$. The received beat signal from a point target can be expressed as

$$S_r(t) = A_0 \mathrm{rec}\,(t/T_o)\cos(2\pi f_b t + \varphi_0) \tag{1}$$

for $-T_o/2 < t < T_o/2$, where A_0 is the received amplitude, f_b the target beat-frequency, φ_0 an arbitrary initial phase. As depicted in Fig. 1(b), the target range is defined as

$$r = \frac{f_b T_o c}{2B_e} \tag{2}$$

where c is the speed of light and B_e the effective bandwidth. The effective bandwidth is related to the transmitted on by

$$B_e = B\left(\frac{T_o}{T_s}\right). \tag{3}$$

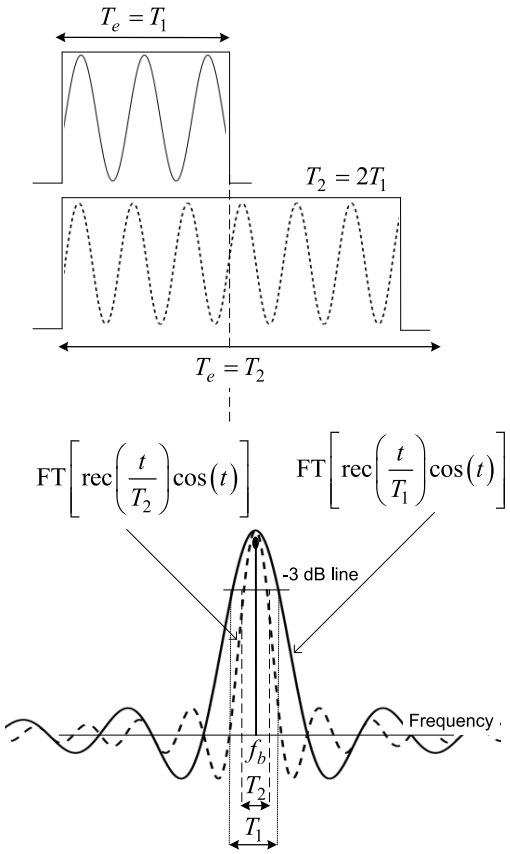

Fig. 2. Simplified sinc function spectral bandwidth illustration for signals with different durations. When coherently concatenating two sweeps, the sinc function 3 dB width will reduce.

which also expresses the degradation in the transmitted bandwidth due to the reduced observation time. From (2), the target beat-frequency is therefore

$$f_b = \frac{2B_e r}{T_o c}. \tag{4}$$

Spectral estimation techniques such as the FT are typically used to estimate the target frequency, and therefore its range.

It is well known from FT signal processing that for a signal as in (1), the FT will result in an impulse function - assuming that f_b is on a frequency grid point - and a sinc function, and that the frequency spectrum resolution is defined by the 3 dB width of that sinc function centered at f_b [4]. The 3 dB width of the sinc function in the frequency domain is inversely proportional to the signal integration time T_e [2] as

$$\Delta f = \frac{1}{T_e}. \tag{5}$$

This concept is depicted in Fig. 2. In FMCW radar, range resolution is proportional to the frequency spectrum resolution, and is defined by the 3 dB width of the sinc function centered at f_b. From (2), (4) and (5), for two targets r_1 and r_2 to be separable in the frequency domain, they need to meet the requirement

$$\frac{2B_e r_1}{T_o c} - \frac{2B_e r_2}{T_o c} \geq \frac{1}{T_e} \tag{6}$$

which can be simplified to

$$r_1 - r_2 = \Delta R = \frac{c}{\left(\frac{2B}{T_o}\right) T_e}. \tag{7}$$

It should be noted that in typical FMCW processing, $T_o = T_e$, yielding

$$\Delta R = \frac{c}{2B_e} \tag{8}$$

which is the classical form of FMCW range resolution. But as seen in (7), if there were a way to increase the integration time, it would be possible to improve the range resolution.

B. Range Resolution Improvement

The method proposed in Section III increases the integration time in (5) and (7) by coherently concatenating d sweeps, and therefore improving the range resolution. The improved range resolution is expressed as follows

$$\Delta R_d = \frac{c}{\left(\frac{2B_e}{T_o}\right) d T_e} = \frac{c}{2B_e d} \tag{9}$$

where d is the concatenation factor as well as the range resolution improvement factor. It should be noted that the more coherently concatenated sweeps, the finer ΔR_d becomes, and therefore the larger the observed range migration is for moving targets. Range migration is sometimes a desirable phenomenon, where it is exploited for better performance of some detection algorithms [12]. If range migration is not desirable for certain applications, it can be corrected using algorithms like in [13] and [14]. The value of d should therefore become a radar system parameter. We will show in Section II-C and Section III that different size slow-time fast-time matrices can be created in parallel from a single CPI, by processing for different values of d.

C. Reconfigurable Range-Doppler Processing

In classical FMCW radar processing, a CPI of a certain duration is selected as a system parameter. Received sweeps in the CPI are typically stored in a 2-D matrix (commonly named the fast-time slow-time matrix), after which, a 2-D FT is performed on that matrix to produce range-Doppler maps. The total processing gain in the CPI is the pulse compression gain - also known as the time-bandwidth product (BT) - multiplied by the number of sweeps in the CPI. Operationally, to maintain this processing gain, the total number of samples stored in a CPI is typically kept the same when changing the PRF, and a tradeoff is made between the unambiguous range and the unambiguous Doppler velocity interval. This is in the sense that more sweeps of shorter durations are received in High PRF (HPRF) mode, and less sweeps of longer duration in low PRF mode. If the radar operates in a HPRF mode, different unambiguous Doppler velocity intervals can be created by simply discarding every other sweep(s) in the fast-time slow-time matrix, but that would result in a total processing gain loss. The unambiguous velocity interval is related to the PRF as

$$v_u = \pm\frac{\lambda \cdot \mathrm{PRF}}{4} \tag{10}$$

TABLE I

FLEXIBLE CPI PROCESSING RANGE RESOLUTION IMPROVEMENT VS MAXIMUM UNAMBIGUOUS DOPPLER VELOCITY TRADEOFF EXAMPLE. ASSUMPTIONS ARE: TRANSMITTED PRF = 2kHz, $T_s = 500\ \mu$s, $T_o = 400\ \mu$s, $N = 64$ SWEEPS IN THE CPI, CPI LENGTH = 32000 μs, $B_e = 32$ MHz, WAVELENGTH $\lambda = 0.0905$ m. NOTE THAT WHEN $d = 1$, THIS IS THE CASE FOR CONVENTIONAL PROCESSING

Concatenation Factor d	Range Processing Gain $G_r = B_e T_o d$	Range Resolution $\Delta R_d = \frac{c}{2B_e d}$ (m)	N CPI Doppler Processing Gain	Total CPI Processing Gain = Range Processing Gain x N CPI Doppler Processing Gain	Processing PRF (kHz)	Maximum Unambiguous Doppler Velocity $v_u = \pm\frac{\lambda \cdot \mathrm{PRF}}{4}$ (m/s)
1	12800	4.68	64	819200	2	45.25
2	25600	2.34	32	819200	1	22.62
4	51200	1.17	16	819200	0.5	11.31
.	.	.	.	.	.	.
.	.	.	.	.	.	.
64	819200	0.07	1	819200	Not applicable.	Not applicable. Only a range profile is available.

where λ is the radar wavelength. We propose the creation of different lengths fast-time slow-time matrices by operating the radar in a HPRF mode, and concatenating sweeps for different values of d in parallel. This will allow the creation of different 'processing' PRF values from the operational HPRF, while maintaining the total processing gain. The created different processing PRF values will allow for the evaluation of multiple unambiguous Doppler velocity intervals, and multiple range resolution granularities, from the same CPI. The processing PRF can be expressed as

$$\mathrm{PRF}_d = \frac{\mathrm{PRF}}{d}. \tag{11}$$

This reconfigurable processing concept is illustrated in Fig. 3, where as the number of concatenated sweeps increase, the unambiguous Doppler velocity intervals is reduced, but all samples are still used and therefore the processing gain is maintained.

A calculated example is furthermore given in Table I. It can be seen that when $d = 2$ for instance, the processing PRF becomes 1 kHz, which is half the transmitted PRF of 2 kHz, but the range resolution is improved by a factor of two from 4.68 m to 2.34 m. All while maintaining the same total processing gain of 819200 in both cases because of not discarding any samples.

D. Reconfigurable Range-Doppler Processing Limitations

The limitations for improving the range resolution by coherently concatenating multiple sweeps are system non-linearities - in the transmitter and receiver - and concatenation errors. Because of non-linearities, even a point-target will have a certain 3 dB spectral width, dictated by the radar's non-linearities [15]. Any concatenation errors may also result in grating-lobes or spectral width widening.

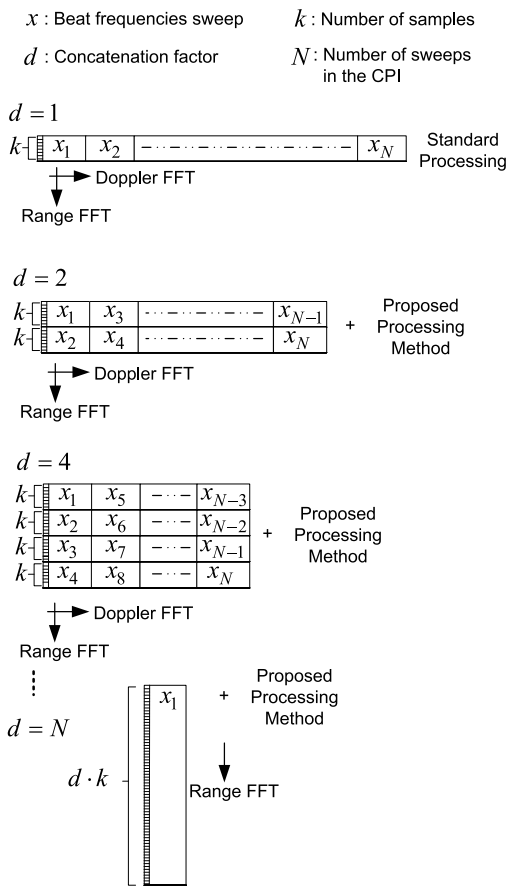

Fig. 3. Reconfigurable range-Doppler processing permutations of fast-time slow-time received sweeps. The total CPI processing gain is maintained. Depending on the number of sweeps concatenated, there is a tradeoff between range resolution and the maximum unambiguous Doppler velocity interval. Note that when $d = N$, only a range profile is provided because the matrix is then one dimensional.

III. METHOD: SWEEPS CONCATENATION WITH TRANSIENT REGION EXTRAPOLATION

In the time-frequency domain, beat-frequency slices are first extrapolated to cover the transient region between sweeps, and then coherently concatenated using a phase-shift operation, as depicted in Fig. 4. The steps are:

1) Store digitally sampled beat-frequencies for sweeps from the output of the deramping receiver. A sweep can be expressed as $x_n[k]$, where n is the sweep number, and $2 \leq n \leq N$. The number of sweeps in a conventional Coherent Processing Interval (CPI) is N, and $N \in \mathbb{N}$, and $\mathbb{N}$ denotes the set of all natural numbers. The time domain sample index in a sweep is k, where

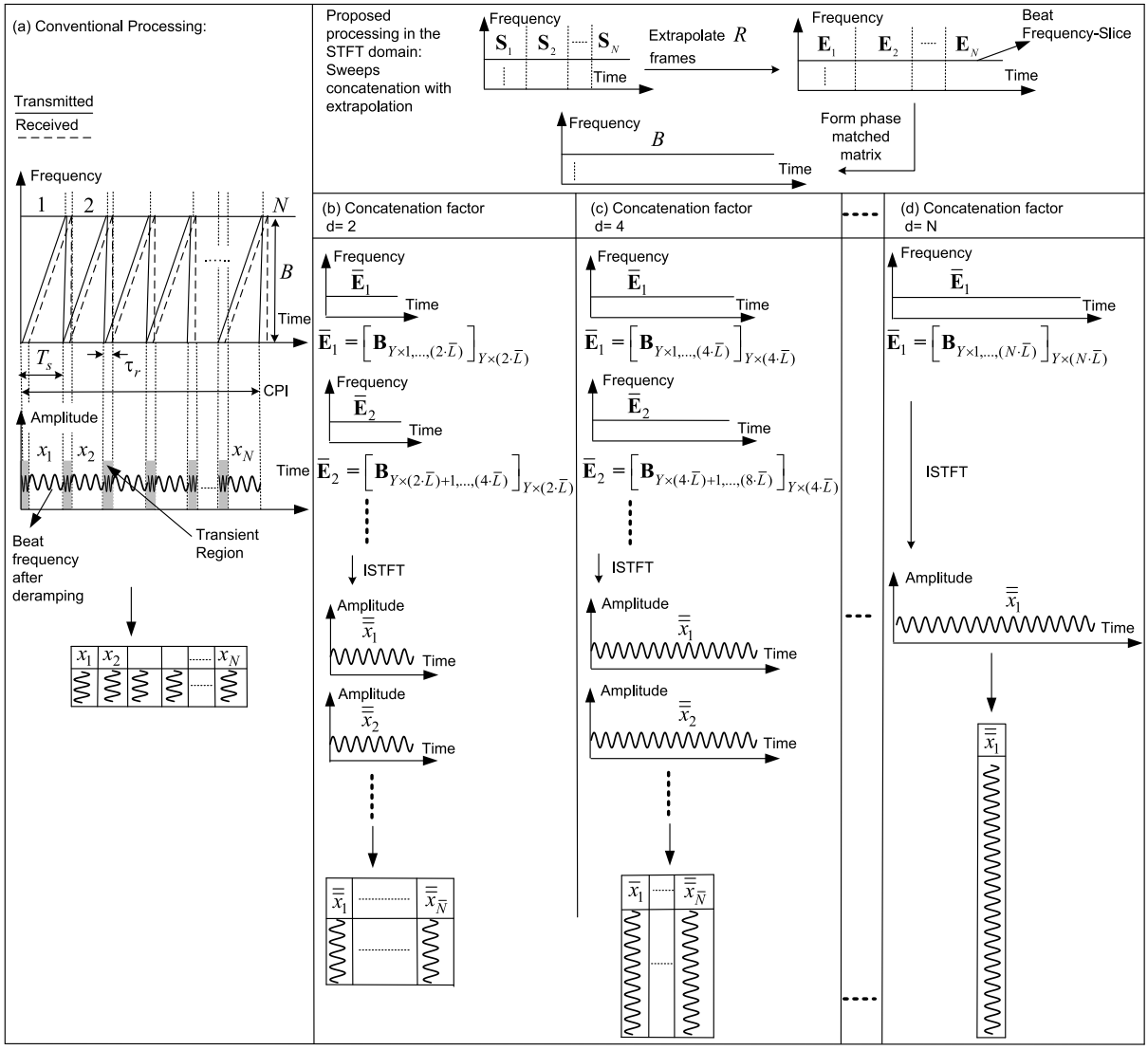

Fig. 4. Examples for reconfigurable CPI processing with transient region frames extrapolation. Different values of the concatenation factor d are shown for sweep concatenation.

$k = 1, \ldots, K$, and $K = f_s T_o$. The sampling frequency is f_s.

2) Take sweeps to the time-frequency domain by applying an STFT, where a sweep can be expressed in matrix form as

$$\mathbf{S}_n[l, y] = \left[\sum_{q=-\frac{W}{2}}^{\frac{W}{2}-1} x[q] w[q - l\Delta h] e^{-i2\pi q y / W} \right]_{Y \times L} \quad (12)$$

with Y rows and L columns, where l is the STFT frame index, $l = 1, \ldots, L$, and $L = 1 + \lfloor (k - W)/\Delta h) \rfloor$. The analysis window length is W. The STFT hop size is Δh, and $\lfloor \cdot \rfloor$ denotes the floor operation. The frequency-slice index in the STFT frequency grid is y, where $y = 0, \ldots, Y$, and Y is the maximum beat-frequency index. The analysis window (for instance, Hamming) is w.

3) Using the Burg algorithm [16], estimate in-phase and quadrature (IQ) Linear Prediction (LP) coefficients $[\mathbf{a}]_{Y \times o}$ in matrix form for amplitudes of each frequency-slice y in each of the N sweeps. The prediction filter order is o, and o should be between 2 and $\lfloor L/3 \rfloor$.

4) Extrapolate R frames for each y frequency-slice, for each of the N sweeps. Note that $R = 1 + \lfloor ((\tau_r f_s) - W)/\Delta h) \rfloor$, and the extrapolated frames can be written as

$$\mathbf{A}_y[r] = \left[\sum_{i=1}^{o} \mathbf{a}_{y,i} \mathbf{S}_{y,i} \right]_{1 \times R} \quad (13)$$

where $r = 1, \ldots, R$. After extrapolating for all y frequency-slices, an extrapolated sweep can then be written as

$$\mathbf{E}_n = \left[\mathbf{A}_n \quad \mathbf{S}_n \right]_{Y \times \bar{L}} \quad (14)$$

where $\bar{L} = L + R$. Note that If the radar is to operate with long delays between sweeps (similarly to pulse-Doppler radar), steps 3 and 4 can be skipped because of the extrapolation quality degradation.

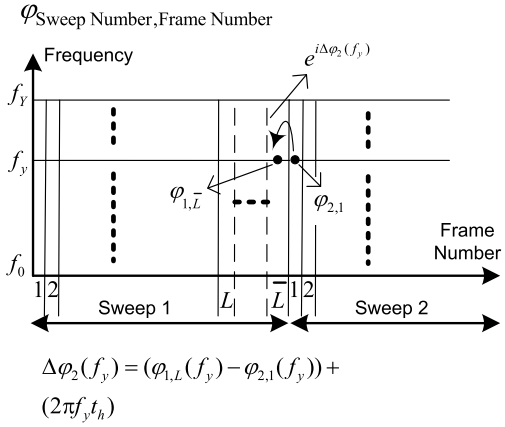

Fig. 5. Depiction of phase matching in the STFT domain after transient region frames extrapolation, as discussed is Section III.

5) Form concatenated sweeps in matrix-form in the STFT domain as:

$$\mathbf{B} = [\,\mathbf{E}_1 \quad \mathbf{E}_2 \circ \mathbf{C}_2 \quad \ldots \quad \mathbf{E}_N \circ \mathbf{C}_N\,]_{Y\times(N\cdot\bar{L})} \tag{15}$$

the $\mathbf{E}$ matrices are of the form as in (14), '$\circ$' denotes the Hadamard product. The phase matching term $\mathbf{C}$ has $\bar{L}$ identical columns, and is defined as

$$\mathbf{C}_i = \begin{bmatrix} e^{i\Delta\varphi_i(f_0)} & \ldots & e^{i\Delta\varphi_i(f_0)} \\ \vdots & \vdots & \vdots \\ e^{i\Delta\varphi_i(f_Y)} & \ldots & e^{i\Delta\varphi_i(f_Y)} \end{bmatrix}_{Y\times\bar{L}} \tag{16}$$

where

$$\Delta\varphi_i(f_y) = (\varphi_{i-1,\bar{L}}(f_y) - \varphi_{i,1}(f_y)) + (2\pi\, f_y t_h). \tag{17}$$

Here f_y is the frequency value at frequency-slice index y, and the hop time $t_h = \Delta h / f_s$. The phase matching is illustrated in Fig. 5.

6) Select a concatenation factor d which indicates the desired number of sweeps to be concatenated in the CPI, where $d \in \mathbb{Q}$, and $\mathbb{Q}$ denotes the set of all rational numbers. The concatenated sweep number is $\overline{N}$, where $\overline{N} = N/d$, and $\overline{N} \in \mathbb{N}$.
7) Form concatenated sweeps in matrix-form in the STFT domain as

$$\bar{\mathbf{E}}_m = [\mathbf{B}_{Y\times((m-1)\cdot d\cdot\bar{L})+1),\ldots,(m\cdot d\cdot\bar{L})}]_{Y\times(d\cdot\bar{L})} \tag{18}$$

where m is the sweep number after concatenation, $m = 1, \ldots, \overline{N}$.
8) Perform an Inverse STFT (ISTFT) to form the new concatenated beat-frequency sweeps as

$$\bar{\bar{x}}_m = \mathrm{ISTFT}(\bar{\mathbf{E}}_m). \tag{19}$$

The concatenated sweep $\bar{\bar{x}}_m$ will be of length $d \cdot (k + (f_s \tau_r))$.
9) Perform again from step 6 onwards in parallel for different values of d to create multiple fast-time slow-time matrices from the same CPI.

TABLE II
SIMULATION AND EXPERIMENT SETUP PARAMETERS

Simulated Targets' Specifications				
Target Number	Range (m)	Velocity (m/s)		
G1	348.28	13.85		
G2	362.98	1.38		
G3	364.45	1.38		
G4	379.14	0		
G5	380.61	0		
CPI Parameters				
Parameter	Value		Unit	
	Simulation	Experiments		
Waveform	Linear sawtooth		n/a	
PRF	1	2	KHz	
T_s	1000	500	μs	
T_o	950	450	μs	
N CPI	64		sweeps	
CPI length	0.064	0.033	s	
B_e	49.5	R-1: 38 R-2: 19	MHz	
wavelength λ	0.0905		m	
Extrapolation Parameters				
Parameter	Value		Unit	
	Simulation	Experiments		
Window length W	8192	6144	samples	
Hop size Δh	8	3	samples	
Extrapolation filter order o	120		coefficients	
Flexible Range-Doppler Processing				
Concatenation Factor	Range Resolution ΔR_d (m)		Maximum Unambiguous Doppler Velocity v_u (m/s)	
	Simulation	Experiments	Simulation	Experiments
d = 1 (standard)	3.02	R-1: 3.74 R-2: 7.49	± 22.1	± 44.4
d = 2	1.46	R-1: n/a R-2: 3.60	± 11	± 22.16
d = 4	0.73	n/a	± 5.5	± 11.08

IV. SIMULATION RESULTS FOR PROPOSED METHOD

To evaluate the reconfigurable range-Doppler and range resolution improvement method, a simulation and processing scenario for five point-targets is setup using the parameters in Table II and illustrated in Fig. 6. On the one hand, the simulation compares 2-D FT results for the standard case with a PRF of 1 kHz (Fig. 6(a)), the creation of a second Doppler velocity ambiguity interval by manually discarding every other sweep from the CPI resulting in a Doppler sampling PRF of 500 Hz (Fig. 6(b)), and the creation of a third interval by manually using one sweep from every four sweeps from the CPI resulting in a Doppler sampling PRF of 250 Hz (Fig. 6(c)). On the other hand this is compared with the proposed processing with $d = 2$ (Fig. 6(d)) and $d = 4$ (Fig. 6(e)) to create the same velocity ambiguity intervals, but with improving the range resolution. Hamming windowing is used for both the range and Doppler processing. The simulation results are presented in Fig. 7. Target G1 wraps around the unambiguous velocity intervals as expected, as it can be seen at a velocity of around -9 m/s in Fig. 7(b) and (d), and at around 3 m/s in Fig. 7(c) and (e). Targets G2 and G3 have a velocity which is always within the ambiguity intervals, and therefore do not fold. Since targets G2 and G3 are spaced 1.5 meters apart,

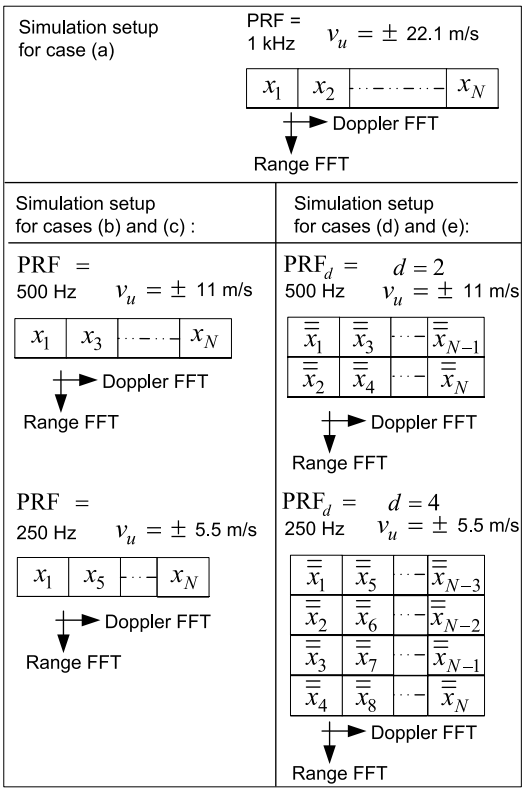

Fig. 6. Simulation setup for the results presented in Fig. 7, where cases (a) to (e) correspond to Fig. 7 sub-figure labels.

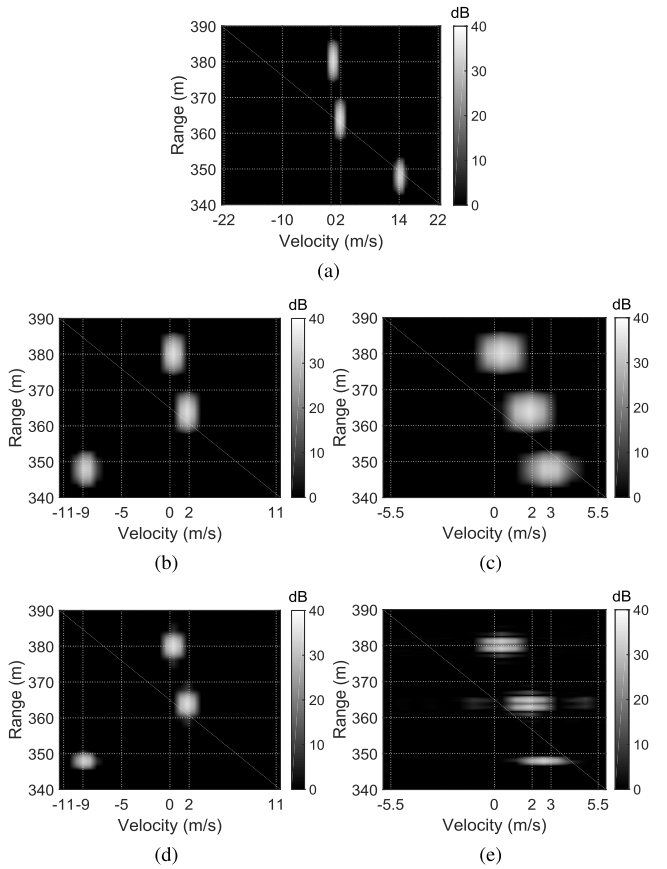

Fig. 7. Simulation Results for the scenario setup using the parameters in Table II and illustrated in Fig. 6. (a) Standard processing, PRF = 1 kHz. (b) Dropped sweeps to create PRF = 500 Hz. (c) Dropped sweeps to create PRF = 250 Hz. (d) Proposed processing with $d = 2$. (e) Proposed processing with $d = 4$.

they are only distinguishable when processing with $d = 4$, because the improved range resolution is then 0.73 m, as seen in Fig. 7(e). This resolvability is also the case for targets G4 and G5 which are at zero velocity.

V. Experimental Verification

A. Experimental Setup

The reconfigurable processing and range resolution improvement method is demonstrated experimentally using the Delft University of Technology (TU Delft) PARSAX FMCW radar [17] shown in Fig. 8(a). The radar is mounted on the roof of the electrical engineering, mathematics and computer science (EEMCS) building at the TU Delft. It operates in S-band (3.1315 GHz) and uses an Intermediate Frequency (IF) of 125 MHz. A simplified PARSAX block diagram is depicted in Fig. 9 along with the experimental setup. On every receiver channel, transmitted and received signals are sampled at IF using a pair of Analog-to-Digital Converters (ADCs) on an Innovative Integrations X5-400M Xilinx Virtex5SX95T FPGA card. The ADCs are 14-bit devices with sampling rates up to 400 Mega Samples per Second (MSPS). Deramping Single-Sideband (SSB) signal processing is performed digitally on the FPGAs. Beat-frequencies are transferred to a computer via the PCI-express bus for further processing. Experiments were conducted using the experiments-applicable configuration options shown in Table II. The transmitted waveform from the AWG channel-1 was created by combining two frequency slopes of bandwidths 40 MHz and 20 MHz respectively. Receivers R-1 and R-2 separate the received beat-frequencies from the

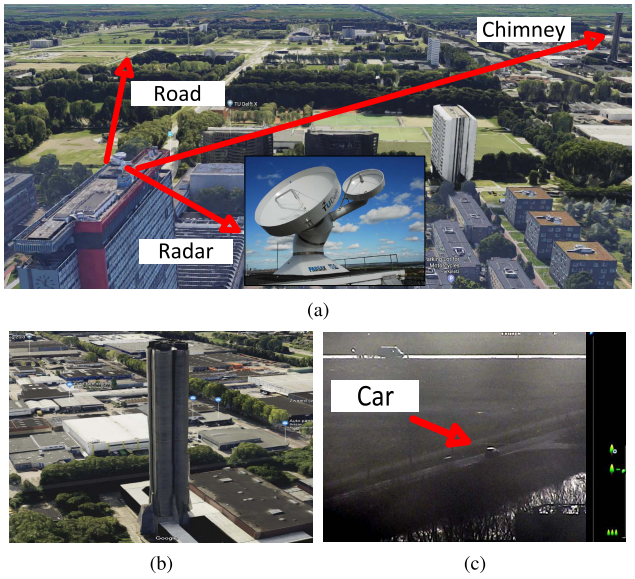

Fig. 8. (a) The PARSAX FMCW radar situated at the top of the TU Delft building was used for the experiments. (b) Industrial chimney used as a stable target in the first experiment. (C) An automobile used as a moving target in the second experiment.

40 MHz and 20 MHz respectively. Both receivers are SSB IQ ones, with the ability to reject either positive or negative frequencies.

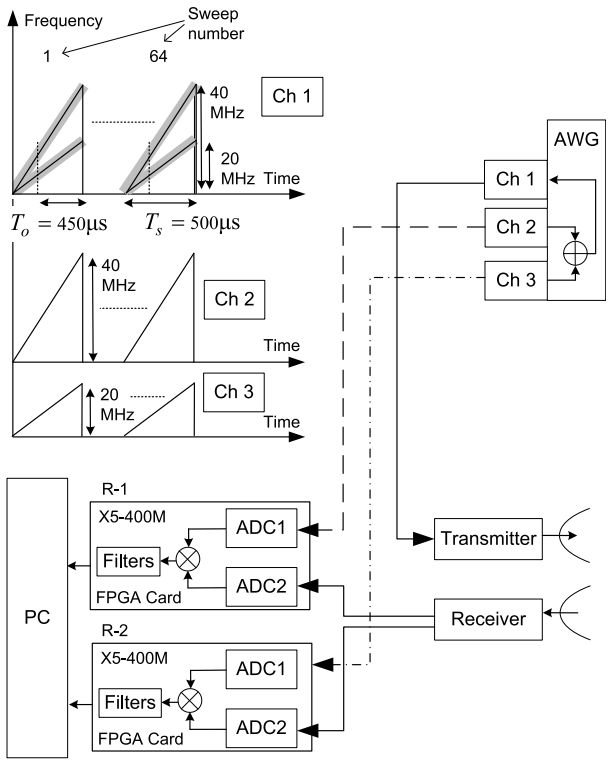

Fig. 9. Simplified PARSAX radar block diagram with the configuration used for experiments discussed is Section V. A waveform combining a 20 MHz and a 40 MHz sweeps is generated and combined by the Arbitrary Waveform Generator (AWG). Both FPGA receivers R-1 and R-2 are SSB IQ ones, with the ability to reject either positive or negative frequencies. The shaded areas depict the receivers' upper and lower LPF bounds.

The aim here is to demonstrate that the range resolution from processing the 20 MHz waveform can be improved to match that of the 40 MHz one, using the proposed method with a concatenation factor $d = 2$.

B. Experiment 1: A Stable Target

In this experiment we observe an industrial factory chimney as depicted in Fig. 8(a) and (b). The chimney is chosen as a stable target. The chimney is made up of multiple sub-chimneys.

C. Experiment 2: A Moving Target

In this experiment, we observe an automobile on a quiet road as depicted in Fig. 8(a) and (c). The automobile driving at a velocity of around 19 m/s (70 kmh) will be unambiguous for the transmitted PRF of 2 kHz, and for when processing with a concatenation factor $d = 2$, which will reduce the processing PRF to 1 kHz.

D. Results and Discussion

For the first experiment, the results are shown in Fig. 10. When processing the 20 MHz waveform with a concatenation factor $d = 2$, the results closely match that of the 40 MHz waveform. The sub-chimneys are resolvable, as can be seen in the disbalanced shape of the sinc-function in Fig. 10. This resolvability is confirmed by the measurement using

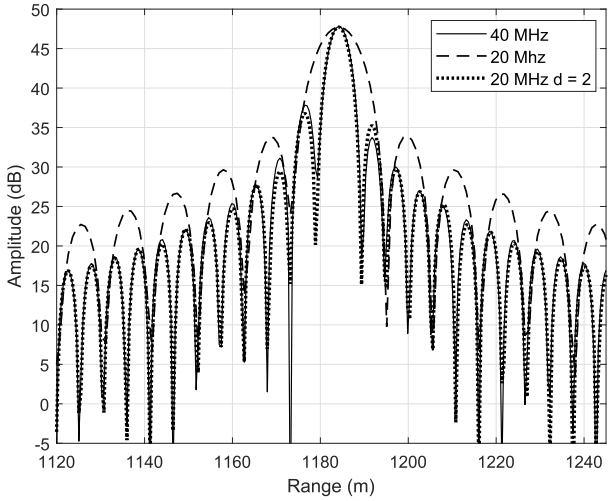

Fig. 10. Zero-Doppler cut zoom-in on the Chimney shown in Fig. 8 (a) and (b). The proposed processing of the 20 MHz channel - with a concatenation factor $d = 2$ - closely matches that of the 40 MHz channel. The sub-chimneys are resolvable, as can be seen in the disbalanced shape of the sinc-function.

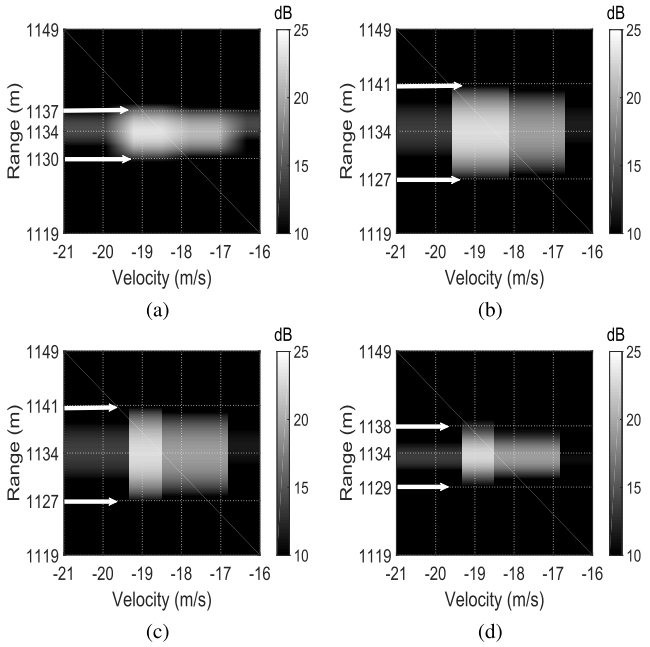

Fig. 11. Range-Velocity results maps for the automobile in the experiment described in Section. V-C. (a) As seen in the 40 MHz channel. (b) As seen in the 20 MHz channel. (c) Processing with manually discarding every other sweep of the 20 MHz channel. (d) Processing the 20 MHz waveform with a concatenation factor $d = 2$, the automobile's resolution closely match that of the 40 MHz waveform, in range, velocity and SNR.

the 40 MHz bandwidth waveform, in comparison with the proposed method being used on the 20 MHz waveform. For the second experiment, the results are shown in Fig. 11. The automobile appears to be of around 7 m in length in the 40 MHz channel, which is expected due to the range resolution being 3.74 m (as seen in Table II), FT leakage, and typical automobile lengths of around 4 m. In the 20 MHz channel, the automobile appears to be of around 14 m in length, which is also expected due to the range resolution being 7.49 m. When processing with manually discarding every other sweep of the the 20 MHz channel, similarly to what was done

in the simulations section, the automobile appears to have the same velocity but with a slight SNR loss and a slight velocity displacement due to the FT leakage. When processing the 20 MHz waveform with a concatenation factor $d = 2$, the automobile's resolution closely match that of the 40 MHz waveform, in range, velocity and SNR.

VI. Conclusion

A reconfigurable range-Doppler processing and range resolution improvement method for FMCW radar was presented. The problem which this paper offered a solution for was the existence of the transient regions in FMCW deramp processing. This region does not allow for longer targets observations, and this limits the maximum range resolution that can be achieved. The solution proposed in this paper was to coherently concatenate beat-frequency slices in the STFT domain, by applying a phase correction to each frequency slice as appropriate, followed by an Inverse STFT (ISTFT). The method extends the observation time by using returns from more than one sweep at a time, which resulted in a finer range resolution without the need to transmit additional bandwidth. The method also made it possible to decouple the Doppler processing PRF from the transmitted signal PRF. This is in the sense that it became possible to - in parallel and from one CPI - create different lengths fast-time slow-time matrices, which allows the observation of different range resolution granularities, without compromising on the total processing gain in any of the created matrices. This therefore also allows for the observation of different unambiguous Doppler velocity intervals (to implement staggered-PRF velocity disambiguation techniques for example) in a single CPI.

Acknowledgment

The authors would also like to thank Fred van der Zwan for his assistance with the measurements.

References

[1] A. G. Stove, "Linear FMCW radar techniques," *IEE Proc. Radar Signal Process.*, vol. 139, no. 5, pp. 343–350, Oct. 1992.
[2] J. D. Watson and N. B. Jones, *Digital Signal Processing: Principles, Devices and Applications*. Stevenage, U.K.: Institution of Electrical Engineers, 1990.
[3] D. E. Barrick, "FMCW radar signals and digital processing," NOAA, Silver Spring, MI, USA, Tech. Rep. ERL 283-WPL 26, 1973.
[4] M. A. Richards, *Fundamentals of Radar Signal Processing*, 2nd ed. New York, NY, USA: McGraw-Hill, 2014.
[5] E. D. Adler, E. A. Viveiros, T. Ton, J. L. Kurtz, and M. C. Bartlett, "Direct digital synthesis applications for radar development," in *Proc. Int. Radar Conf.*, May 1995, pp. 224–226.
[6] Y. Li and S. O'Young, "Method of doubling range resolution without increasing bandwidth in FMCW radar," *Electron. Lett.*, vol. 51, no. 12, pp. 933–935, Nov. 2015.
[7] V. K. Nguyen and M. D. Turley, "Bandwidth extrapolation of LFM signals for narrowband radar systems," in *Proc. Int. Conf. Radar*, Sep. 2013, pp. 140–145.
[8] K. Suwa and M. Iwamoto, "A bandwidth extrapolation technique of polarimetric radar data and a recursive method of polarimetric linear prediction coefficient estimation," in *Proc. IEEE Int. Geosci. Remote Sens. Symp.*, vol. 7, Jul. 2003, pp. 4329–4331.
[9] K. Suwa and M. Iwamoto, "A two-dimensional bandwidth extrapolation technique for polarimetric synthetic aperture radar images," *IEEE Trans. Geosci. Remote Sens.*, vol. 45, no. 1, pp. 45–54, Jan. 2007.
[10] A. Lulu and B. G. Mobasseri, "Phase matching of coincident pulses for range-Doppler estimation of multiple targets," *IEEE Signal Process. Lett.*, vol. 26, no. 1, pp. 199–203, Jan. 2019.
[11] S. Neemat, O. Krasnov, and A. Yarovoy, "An interference mitigation technique for FMCW radar using beat-frequencies interpolation in the STFT domain," *IEEE Trans. Microw. Theory Techn.*, vol. 67, no. 3, pp. 1207–1220, Mar. 2018.
[12] N. Petrov, F. L. Chevalier, and A. G. Yarovoy, "Detection of range migrating targets in compound-Gaussian clutter," *IEEE Trans. Aerosp. Electron. Syst.*, vol. 54, no. 1, pp. 37–50, Feb. 2018.
[13] F. Uysal and N. Goodman, "The effect of moving target on range-Doppler map and backprojection algorithm for focusing," in *Proc. IEEE Radar Conf. (RadarConf)*, May 2016, pp. 1–5.
[14] F. Uysal, "Comparison of range migration correction algorithms for range-Doppler processing," *J. Appl. Remote Sens.*, vol. 11, no. 3, 2017, Art. no. 036023.
[15] M. Jankiraman, *Design of Multi-Frequency CW Radars*. Rijeka, Croatia: SciTech, 2007.
[16] S. Kay, *Modern Spectral Estimation: Theory Application*. Upper Saddle River, NJ, USA: Prentice Hall, 1999.
[17] O. A. Krasnov, L. P. Ligthart, Z. Li, G. Babur, Z. Wang, and F. van der Zwan, "PARSAX: High-resolution Doppler-polarimetric FMCW radar with dual-orthogonal signals," in *Proc. 18th Int. Conf. Microw. Radar Wireless Commun. (MIKON)*, Jun. 2010, pp. 1–5.

Sharef Neemat received the B.S. degree in computer engineering from King Saud University (KSU) and the M.Sc. degree in electrical engineering from the University of Cape Town (UCT). He is currently pursuing the Ph.D. degree with the Microwave Sensing, Signals and Systems (MS3) Section, Faculty of Electrical Engineering, Mathematics, and Computer Science (EEMCS), Delft University of Technology, Delft, The Netherlands. His study focused on secondary surveillance radar (SSR) identification friend or foe (IFF).

Before and after receiving his M.Sc. degree, he was involved in airborne radios work in the form of design, development, and test of field-programmable gate array (FPGA)/digital signal processor (DSP) drivers and application layer SW for radio housekeeping and scheduling. The DSP designs and code were developed to comply with DO-178B level C (Software Considerations in Airborne Systems and Equipment Certification) and MISRA (Motor Industry Software Reliability Association C Standard). He was also responsible for system engineering/project management of asset-tracking-systems' development. The work had involved writing system engineering management plans and requirements documentation for systems and their subsystems, complying with MIL-STD-490 and MIL-STD-491.

Faruk Uysal (SM'16) received the M.S. and Ph.D. degrees in electrical engineering from New York University (NYU), NY, USA, in 2010 and 2016, respectively.

During his study, Dr. Uysal focused on signal separation techniques for dynamic clutter mitigation. From 2011 to 2014, he was a Staff Engineer with C&P Technologies, Inc., Closter, NJ, USA. He was a Radar Engineer with the Advanced Radar Research Center (ARRC), The University of Oklahoma, Norman, OK, USA, from 2014 to 2016, where he worked on the design and implementation of various projects of the Department of Defense (DoD) Agencies. In 2016, he joined the Microwave Sensing, Signals and Systems (MS3) Section, Faculty of Electrical Engineering, Mathematics, and Computer Science (EEMCS), Delft University of Technology, as an Assistant Professor. He is also an Affiliate Member of the Advanced Radar Research Center (ARRC), The University of Oklahoma. His current research interests include radar signal processing, waveform design, beamforming, radar image formation, clutter mitigation, cognitive radar, and distributed radar systems. Dr. Uysal currently serves as a Reviewer for the IEEE Transactions on Aerospace and Electronic Systems, the IEEE Transactions on Geoscience and Remote Sensing (TGARS), and the *Journal of Applied Remote Sensing* (SPIE).

Oleg Krasnov received the M.S. degree in radio physics from Voronezh State University, Russia, in 1982, and the Ph.D. degree in radio technique from the National Aerospace University "Kharkov Aviation Institute," Ukraine, in 1994.

In 1999, he joined the International Research Center for Telecommunications and Radar (IRCTR), TU Delft. Since 2009, he has been a Senior Researcher with the Microwave Sensing, Signals and Systems (MS3) Section, Faculty of Electrical Engineering, Mathematics, and Computer Science (EEMCS), Delft University of Technology, where he became a Universitair Docent (Assistant Professor) in 2012. His research interests include radar waveforms, signal and data processing algorithms for polarimetric radars and distributed radar systems, multisensor atmospheric remote sensing, and optimal resource management of adaptive radar sensors and distributed systems. Dr. Krasnov has served as the Secretary of the 9th European Radar Conference (EuRAD12), Amsterdam, The Netherlands.

Alexander Yarovoy (F'15) received the Diploma (Hons.) degree in radiophysics and electronics, the Candidate Phys. and Math.Sci. degree in radiophysics, and the Doctor Phys. and Math.Sci. degree in radiophysics from Kharkov State University, Kharkiv, Ukraine, in 1984, 1987, and 1994, respectively.

In 1987, he joined the Department of Radiophysics, Kharkov State University, as a Researcher, where he became a Professor in 1997. From 1994 to 1996, he was a Visiting Researcher with the Technical University of Ilmenau, Ilmenau, Germany. Since 1999, he has been with the Delft University of Technology, Delft, The Netherlands. Since 2009, he has been the Chair of Microwave Sensing, Signals, and Systems. He has authored or coauthored over 250 scientific or technical papers and 14 book chapters and holds four patents. His current research interests include ultrawideband microwave technology and its applications (particularly radars) and applied electromagnetics (particularly UWB antennas). Prof. Yarovoy was a co-recipient of the European Microwave Week Radar Award for the paper that best advances the state of the art in radar technology in 2001 (together with L. P. Ligthart and P. van Genderen) and in 2012 (together with T. Savelyev) and the Best Paper Award of the Applied Computational Electromagnetic Society in 2010 (together with D. Caratelli). Since 2008, he has been the Director of the European Microwave Association. He has served as the Chair and the TPC Chair of the Fifth European Radar Conference, Amsterdam, The Netherlands, as well as the Secretary of the First European Radar Conference, Amsterdam. He has served as the Co-Chair and the TPC Chair of the Tenth International Conference on Ground Penetrating Radar, Delft. He has served as the Guest Editor of five special issues for the IEEE TRANSACTIONS and other journals. Since 2011, he has been an Associate Editor of the *International Journal of Microwave and Wireless Technologies*.